Sensors and Materials, Vol. 37, No. 2 (2025) 599–605
MYU Tokyo

S & M 3940

Optically and Thermally Stimulated Luminescence Properties of Mn-doped CaB_2O_4 Crystals for Neutron Detection

Hiromi Kimura,[1*] Takeshi Fujiwara,[1] Hidetoshi Kato,[1] Masanori Koshimizu,[2]
Genichiro Wakabayashi,[3] Yuma Takebuchi,[4] Takumi Kato,[5]
Daisuke Nakauchi,[5] Noriaki Kawaguchi,[5] and Takayuki Yanagida[5]

[1]National Metrology Institute of Japan, National Institute of Advanced Industrial Science and Technology (AIST), 1-1-1 Umezono, Tsukuba, Ibaraki 305-8568, Japan
[2]Research Institute of Electronics, Shizuoka University, 3-5-1 Johoku, Chuo-ku, Hamamatsu 432-8011, Japan
[3]Atomic Energy Research Institute, Kindai University, 3-4-1 Kowakae, Higashiosaka, Osaka 577-8502, Japan
[4]Faculty of Engineering, Utsunomiya University, Utsunomiya, Tochigi 321-8585, Japan
[5]Division of Materials Science, Nara Institute of Science and Technology (NAIST), 8916-5 Takayama, Ikoma, Nara 630-0192, Japan

(Received October 31, 2024; accepted Decemeber 23, 2024)

Keywords: storage phosphors, thermally stimulated luminescence, photoluminescence, neutron detectors

0.01, 0.1 and 0.5% Mn-doped CaB_2O_4 (CBO) crystals were grown by the floating zone technique and investigated in terms of their structurally, optically, and thermally stimulated luminescence (TSL) properties. Under an excitation of 405 nm, a broad emission peak due to the d-d transitions of Mn^{2+} was observed in all the Mn-doped CBO crystals. Regarding the TSL properties, TSL glow curves were observed with and without Cd filters after neutron irradiations. All the Mn-doped CBO crystals showed an increase in TSL intensity linearly proportional to neutron fluence in the range of 1.0×10^9–1.0×10^{11} neutrons/cm^2.

1. Introduction

Storage phosphors absorb and store part of incident radiation energy. When exposed to ionizing radiation, a lot of carriers were generated and captured by trapping centers within the material. The trapped carriers can be released by thermal or optical stimulation to emit photons. The luminescence obtained by thermal and optical stimulations are called thermally stimulated luminescence (TSL) and optically stimulated luminescence (OSL), respectively.[1] Since the TSL or OSL intensity is proportional to the radiation dose in wide dynamic ranges, the storage phosphors have been used for many applications including medicine imaging,[2–6] environmental dosimetry,[7,8] and personal dose monitoring.[9–11] The required properties for storage phosphors depended on the applications. As a result, many kinds of storage phosphors have been developed to meet specific application needs.[12–21]

In recent years, neutrons have been utilized in a variety of techniques including boron neutron capture therapy,[22–24] radioisotope production,[22] elemental analysis,[25] and

*Corresponding author: e-mail: h.kimura@aist.go.jp
https://doi.org/10.18494/SAM5442

ISSN 0914-4935
https://myukk.org/

radiography.[25–27] As the applications of neutrons expand, there is a demand for the development of neutron detectors with high sensitivity and a wide dynamic range. Since neutrons cannot directly cause ionization, they are indirectly detected by converting them into high-energy photons or charged particles through nuclear reactions with several nuclides including ^{3}He, ^{6}Li, and ^{10}B. To date, borate-based phosphors have attracted much attention as TSL phosphors for dosimetry because they have good tissue equivalence and sensitivity to neutrons.[28–30] Among them, rare-earth- and transition-metal-ion-doped calcium borate components such as CaB_2O_4 (CBO), $Ca_2B_2O_5$, and CaB_4O_7 were reported by many researchers, and they have shown intense TSL after beta-ray or X-ray irradiation.[31–36] However, there are only a few reports on their neutron detection properties as TSL materials, and the available reports on TSL properties analyzed after neutron irradiation are primarily limited to Tb- or Dy-doped $Ca_2B_2O_5$ ceramics.[35,36] In this study, we have investigated the optical and TSL properties of Mn-doped CBO crystals after neutron irradiation and evaluated their potential as neutron detectors.

2. Experimental Methods

CBO crystals doped with different Mn concentrations (0.01, 0.1, and 0.5%) were grown by the floating zone (FZ) technique. The raw powders of $CaCO_3$ (Kojundo Chemical Laboratory, 4N), B_2O_3 (Kojundo Chemical Laboratory, 4N), and MnO (Kojundo Chemical Laboratory, 3N) were mixed in a stoichiometric ratio. Here, the natural isotope B_2O_3, which consists of 19.9% ^{10}B and 80.1% ^{11}B, was used. The mixture was formed to a cylindrical shape by cold isostatic pressing at 40 MPa for 5 min and sintered at 800 °C for 8 h using an electric furnace. The prepared ceramic rods were grown using an optical FZ furnace with four ellipsoidal mirrors and halogen lamps. During the crystal growth, the pulling speed and rotation rate were 10 mm/h and 15 rpm, respectively. A photograph of the prepared Mn-doped CBO crystals is shown in Fig. 1.

The crystal structural property was analyzed by X-ray diffraction (XRD) using a diffractometer (Rigaku, MiniFlex400). The optical properties were investigated using the diffuse transmittance spectra, photoluminescence (PL) excitation and emission spectra, and PL decay curves obtained using a spectrophotometer (Shimadzu, SolidSpec-3700), a spectrofluorometer (JASCO, FP-8550), and a Quantaurus-τ (Hamamatsu Photonics, C11367), respectively. As the TSL properties, the TSL glow curves were measured using the original setup.[37] Before the measurements, the CBO crystals were irradiated with neutrons using the

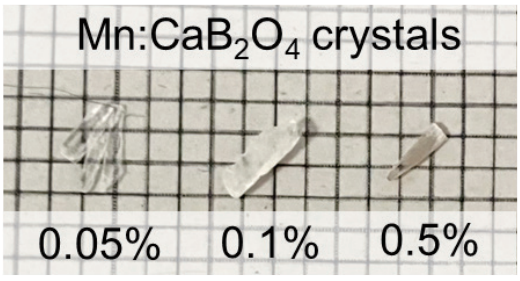

Fig. 1. (Color online) Photograph of prepared 0.05, 0.1, and 0.5% Mn-doped CBO crystals.

UTR-KINKI research reactor at Kindai University, Japan.[38] Here, the neutron irradiation of the crystals was performed with and without Cd filters (~1 mm) because neutron fields are typically present with gamma rays. To investigate the relationship between neutron flux and TSL intensity, the several TSL glow curves were measured at different neutron fluxes of 1.0×10^9, 1.0×10^{10}, and 1.0×10^{11} neutrons/cm^2.

3. Results and Discussion

Figure 2 shows the XRD patterns of Mn-doped CBO crystals. The diffraction peak positions of the prepared Mn-doped CBO crystals are in good agreement with the reference data for the orthorhombic structure of CaB_2O_4. The single phase of CBO was successfully obtained by the FZ technique as no impurity phases were detected.

The diffuse transmittance spectra of Mn-doped CBO crystals are presented in Fig. 3. The 0.05% Mn-doped CBO crystal has a high transmittance of ~80% in the range of 350–850 nm. The transmittance decreased with increasing Mn concentration. The possible reasons would be attributed to the effects of light scattering centers including cracks and voids in the crystal, which would be due to the $(B_2O_4)_n^{2n-}$ layers parallel to the c-axis in the CBO lattice.[39] In all the crystals, the absorption band around 300 nm was observed. Since the absorption intensity increased with increasing Mn concentrations, it may be related to the Mn doping. In the 0.5% Mn-doped CBO crystal, the broad absorption band around 480 nm was observed. Since this absorption band was observed in previous studies on Mn-doped phosphors, it was assigned to the $^6A_1(^6S) \rightarrow {}^4A_1(^4G)/{}^4E(^4G)$ transitions of Mn^{2+}.[40,41]

Figure 4 indicates PL excitation and emission spectra of the Mn-doped CBO crystals. Under an excitation of 405 nm, the emission peak around 530 nm was observed in all the Mn-doped CBO crystals. The emission peak was assigned to the $^4T_1(^4G) \rightarrow {}^6A_1(^6S)$ transitions of Mn^{2+}.[41,42] Additionally, the emission peaks around 600–750 nm were observed in the CBO crystals with Mn concentrations of 0.1% or less. As in the previous reports, the emission peaks at

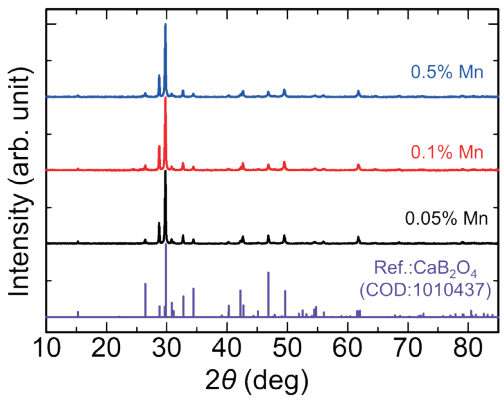

Fig. 2. (Color online) XRD patterns of Mn-doped CBO crystals and standard cards of CBO (COD: 1010437).

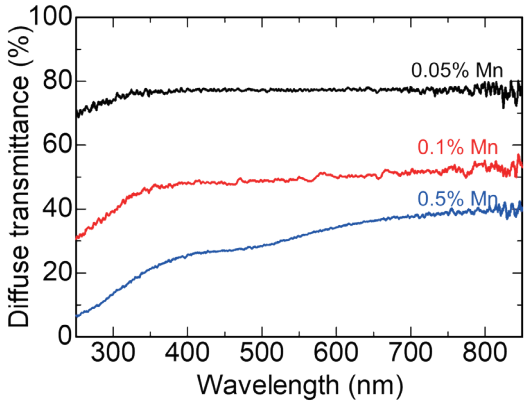

Fig. 3. (Color online) Diffuse transmittance spectra of Mn-doped CBO crystals.

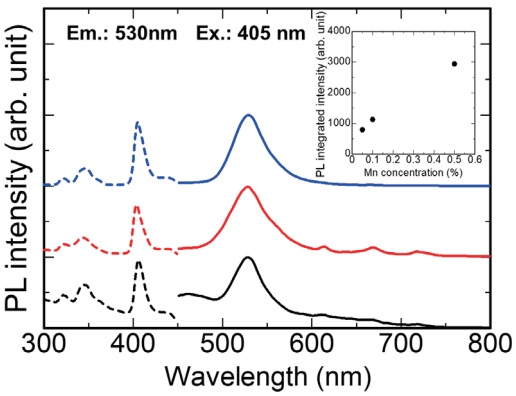

Fig. 4. (Color online) PL excitation (dotted lines) and emission (solid lines) spectra of Mn-doped CBO crystals. The inset shows the PL integrated intensity of the Mn-doped CBO crystals.

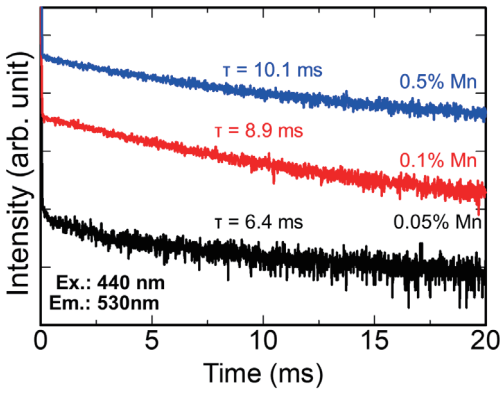

Fig. 5. (Color online) PL decay curves of Mn-doped CBO crystals monitored at 530 nm under excitation of 440 nm.

650 and 710 nm were referred to the charge transfer associated with the Mn^{2+} ion and cation vacancies, respectively.[43–45] The excitation spectra monitored at 530 nm showed several peaks around 320, 350, and 405 nm, which corresponded to the $^4E(^4D)$, $^4T_2(^4D)$, $^4A_1(^4G)/^4E(^4G) \rightarrow {}^6A_1(^6S)$ transitions of Mn^{2+}.[40,46] The inset of Fig. 4 shows the PL integrated intensity of Mn-doped CBO crystals. The integrated range is 500–600 nm for PL spectra. As the Mn concentration increased, the PL intensity increased.

PL decay curves of Mn-doped CBO crystals monitored at 530 nm under an excitation of 440 nm are presented in Fig. 5. All the decay curves of Mn-doped CBO crystals were approximated from a single exponential decay function, and the obtained lifetimes for Mn-doped CBO crystals were 6.4–10.1 ms, which were reasonable for the d-d transitions of Mn^{2+}.[42,47] The lifetimes decreased with increasing Mn concentration, and this trend was consistent with the result of the PL intensities, which was reasonable.

Figure 6 shows TSL glow curves of the Mn-doped CBO crystals with and without Cd filters after neutron irradiation at 1.0×10^{10} neutrons/cm^2. All the Mn-doped CBO crystals showed multiple TSL glow peaks around 100, 150, and 200 °C, which were similar to that of Mn-doped CaB_4O_7.[31] According to previous studies, the peaks around 100 and 150 °C were observed in the non-doped CBO ceramics, and the origins of trapping centers would be some defects in the anion sublattice.[48–51] The shapes of the glow curves changed with and without Cd filters. Here, the neutron fields are typically present with gamma rays. When Cd filters were used, the Mn-doped CBO crystals were irradiated with gamma rays only because the thermal neutrons were effectively absorbed by the Cd filters. Since the TSL intensity of the peak around 200 °C decreased with the Cd filters in comparison with the other peak intensities, the difference in TSL intensity with and without Cd filters was considered to be caused by neutron irradiation. Therefore, the prepared Mn-doped CBO crystals have the potential use for neutron detection.

The relationship between the neutron flux and integrated TSL intensity above 30–400 °C and 170–230 °C in the Mn-doped CBO crystals is shown in Fig. 7. Here, the integration range of

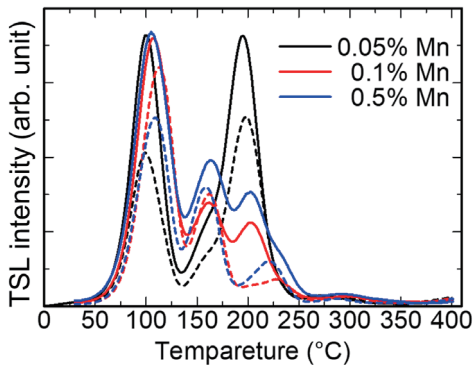

Fig. 6. (Color online) TSL glow curves of Mn-doped CBO crystals with (dotted lines) and without (solid lines) Cd filters after neutron irradiation at 1.0 × 1010 neutrons/cm^2.

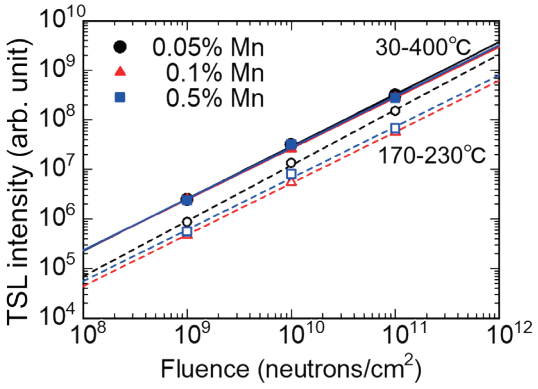

Fig. 7. (Color online) Relationship between neutron flux and integrated TSL intensity above 30–400 °C (solid lines) and 170–230 °C (dotted line) without Cd filters in Mn-doped CBO crystals.

170–230 °C was decided relative to the peaks where there was a significant difference between the data with and without Cd filters. The integrated TSL intensities of all the Mn-doped CBO crystals increased linearly proportionally to neutron fluence in the range of 1.0 × 10^9–1.0 × 10^{11} neutrons/cm^2. In this study, the Mn-doped CBO crystals were synthesized using the raw powder of the natural isotope B_2O_3. Therefore, it is expected that the sensitivity will be improved by using the raw powder of ^{10}B-enriched B_2O_3.

4. Conclusions

The structurally, optically, and TSL properties of 0.01, 0.1, and 0.5% Mn-doped CBO crystals were investigated. Since the XRD patterns were consistent with the reference data for the orthorhombic structure of CBO, all the prepared crystals had the single phase. Under excitations of 320, 350, and 405 nm, the emission peak due to the $^4T_1(^4G) \rightarrow {}^6A_1(^6S)$ transitions of Mn^{2+} was observed. After neutron irradiation using the UTR-KINKI research reactor at Kindai University, all the Mn-doped CBO crystals showed some TSL glow peaks with and without Cd filters. From the difference in TSL intensity, the signal of the glow peak around 200 °C was considered to be caused by neutron irradiation. The TSL signal monotonically increases with the neutron fluence from 1.0 × 10^9 to 1.0 × 10^{11} neutrons/cm^2. Therefore, Mn-doped CBO crystals are suitable as TSL materials for neutron detection.

Acknowledgments

This work was supported by a Grant-in-Aid for Research Activity Start-up (22K20489). The Cooperative Research Project of Shimadzu Science Foundation is also acknowledged. Neutron irradiation using the UTR-KINKI research reactor was performed as part of cooperative research with Kindai University.

References

1 T. Yanagida, G. Okada, and N. Kawaguchi: J. Lumin. **207** (2019) 14.
2 P. Leblans, D. Vandenbroucke, and P. Willems: Materials **4** (2011) 1034.
3 N. Kurata, N. Kubota, Y. Takei, and H. Nanto: Radiat. Prot. Dosimetry **119** (2006) 398.
4 Hidehito Nanto: Sens. Mater. **30** (2018) 327.
5 H. Nanto and G. Okada: Jpn. J. Appl. Phys. **62** (2023) 010505.
6 H. Kimura, T. Kato, T. Fujiwara, M. Tanaka, D. Nakauchi, N. Kawaguchi, and T. Yanagida: Jpn. J. Appl. Phys. **62** (2023) 010504.
7 S. K. Mehta, S. Sengupta, and I.K. Oommen: Nucl. Instruments Methods Phys. Res. **197** (1982) 459.
8 M. Bakr, Z. G. Portakal-Uçar, M. Yüksel, Ü. H. Kaynar, M. Ayvacikli, S. Benourdja, A. Canimoglu, M. Topaksu, A. Hammoudeh, and N. Can: J. Lumin. **227** (2020) 117565.
9 S. W. S. McKeever: Radiat. Meas. **46** (2011) 1336.
10 S. A. Sinclair and M.I. Pech-Canul: Chem. Eng. J. **443** (2022) 136522.
11 T. Kato, D. Nakauchi, N. Kawaguchi, and T. Yanagida: Jpn. J. Appl. Phys. **62** (2023) 010604.
12 M. Koshimizu, K. Oba, Y. Fujimoto, and K. Asai: Sens. Mater. **36** (2024) 565.
13 D. Shiratori, H. Fukushima, D. Nakauchi, T. Kato, N. Kawaguchi, and T. Yanagida: Jpn. J. Appl. Phys. **62** (2023) 010608.
14 S. A. Fartode, A. P. Fartode, and S. J. Dhoble: AIP Conf. Proc. (2019) 020043.
15 S. Chand, R. Mehra, and V. Chopra: Luminescence **36** (2021) 1808.
16 R. Tsubouchi, H. Fukushima, T. Kato, D. Nakauchi, S. Saijo, T. Matsuura, N. Kawaguchi, T. Yoneda, and T. Yanagida: Sens. Mater. **36** (2024) 481.
17 W. Chen and M. Su: Appl. Phys. Lett. **70** (1997) 301.
18 A. Pradhan, J. Lee, and J. Kim: J. Med. Phys. **33** (2008) 85.
19 S. N. Menon, A.K. Singh, S. Kadam, S. Mhatre, B. Sanyal, and B. Dhabekar: J. Food Process. Preserv. **43** (2019) e13891.
20 S. Otake, H. Sakaguchi, Y. Yoshikawa, T. Kato, D. Nakauchi, N. Kawaguchi, and T. Yanagida: Sens. Mater. **36** (2024) 539.
21 N. Kawano, K. Okazaki, Y. Takebuchi, H. Fukushima, T. Kato, D. Nakauchi, F. Kagaya, K. Shinozaki, and T. Yanagida: Jpn. J. Appl. Phys. **62** (2023) 072002.
22 R. F. Barth, J. A. Coderre, M. G. H. Vicente, and T. E. Blue: Clin. Cancer Res. **11** (2005) 3987.
23 K. Shinsho, R. Oh, M. Tanaka, N. Sugioka, H. Tanaka, G. Wakabayashi, T. Takata, W. Chang, S. Matsumoto, G. Okada, S. Sugawara, E. Sasaki, K. Watanabe, Y. Koba, K. Nagasaka, S. Yoshihashi, A. Uritani, and T. Negishi: Jpn. J. Appl. Phys. **62** (2023) 010502.
24 K. Watanabe: Jpn. J. Appl. Phys. **62** (2023) 010507.
25 E. Witkowska, K. Szczepaniak, and M. Biziuk: J. Radioanal. Nucl. Chem. **265** (2005) 141.
26 T. Fujiwara, H. Miyoshi, Y. Mitsuya, N. L. Yamada, Y. Wakabayashi, Y. Otake, M. Hino, K. Kino, M. Tanaka, N. Oshima, and H. Takahashi: Rev. Sci. Instrum. **93** (2022).
27 T. Fujiwara, K. Kino, N. Oshima, and M. Furusaka: Sens. Mater. **35** (2023) 537.
28 M. Prokić: Nucl. Instruments Methods **175** (1980) 83.
29 E. Tekin (Ekdal), A. Ege, T. Karali, P. D. Townsend, and M. Prokić: Radiat. Meas. **45** (2010) 764.
30 R. P. Yavetskiy, E. F. Dolzhenkova, A. V. Tolmachev, S. V. Parkhomenko, V. N. Baumer, and A. L. Prosvirnin: J. Alloys Compd. **441** (2007) 202.
31 K. F. Oguz, E. Ekdal, M. A. A. Aslani, A. Canimoglu, J. Garcia Guinea, N. Can, and T. Karali: J. Alloys Compd. **683** (2016) 76.
32 Y. Fukuda, A. Tomita, and N. Takeuchi: Phys. Status Solidi **85** (1984) K141.
33 Y. Fukuda, A. Tomita, and N. Takeuchi: Phys. Status Solidi **99** (1987) K135.
34 N. K. Porwal, R. M. Kadam, T. K. Seshagiri, V. Natarajan, A. R. Dhobale, and A. G. Page: Radiat. Meas. **40** (2005) 69.
35 H. Komiya, I. Kawamura, H. Kawamoto, Y. Fujimoto, M. Koshimizu, H. Kimura, G. Okada, Y. Koba, T. Yanagida, G. Wakabayashi, and K. Asai: Jpn. J. Appl. Phys. **60** (2021) 092008.
36 H. Komiya, I. Kawamura, H. Kawamoto, Y. Fujimoto, M. Koshimizu, G. Okada, Y. Koba, G. Wakabayashi, and K. Asai: Jpn. J. Appl. Phys. **61** (2022) SB1007.
37 H. Yamaguchi, M. Koshimizu, H. Kawamoto, Y. Fujimoto, G. Wakabayashi, and K. Asai: Radiat. Phys. Chem. **220** (2024) 111703.
38 G. Wakabayashi, T. Yamada, T. Endo, and C. H. Pyeon: Introduction to Nuclear Reactor Experiments (Springer Nature Singapore, Singapore, 2023) pp. 87–123.
39 W. H. Zachariasen: Proc. Natl. Acad. Sci. **17** (1931) 617.

40 K. W. Park, H. S. Lim, S. W. Park, G. Deressa, and J. S. Kim: Chem. Phys. Lett. **636** (2015) 141.
41 A. Tomita, T. Sato, K. Tanaka, Y. Kawabe, M. Shirai, K. Tanaka, and E. Hanamura: J. Lumin. **109** (2004) 19.
42 Y. Takebuchi, H. Fukushima, T. Kato, D. Nakauchi, N. Kawaguchi, and T. Yanagida: J. Mater. Sci. Mater. Electron. **31** (2020) 8240.
43 V. Singh, R. P. S. Chakradhar, J. L. Rao, and D.-K. Kim: J. Solid State Chem. **180** (2007) 2067.
44 J. El Ghoul and L. El Mir: J. Mater. Sci. Mater. Electron. **26** (2015) 3550.
45 N. Pathak, P. S. Ghosh, S. K. Gupta, S. Mukherjee, R. M. Kadam, and A. Arya: J. Phys. Chem. C **120** (2016) 4016.
46 V. Singh, R. P. S. Chakradhar, J. L. Rao, S. J. Dhoble, and S. H. Kim: J. Electron. Mater. **43** (2014) 4041.
47 M. Czaja, R. Lisiecki, R. Juroszek, and T. Krzykawski: Minerals **11** (2021) 1215.
48 I. V. Berezovskaya, N. P. Efryushina, A. S. Voloshinovskii, G. B. Stryganyuk, P. V. Pir, and V. P. Dotsenko: Radiat. Meas. **42** (2007) 878.
49 A. Meijerink, G. Blasse, and M. Glasbeek: J. Phys. Condens. Matter **2** (1990) 6303.
50 Sangeeta and S. Sabharwal: J. Lumin. **104** (2003) 267.
51 Sangeeta and S. Sabharwal: J. Lumin. **109** (2004) 69.